Mesoscale Structure in the Megalopolitan Snowstorm of 11–12 February 1983. Part III: A Large-Amplitude Gravity Wave

LANCE F. BOSART

Department of Atmospheric Science, State University of New York at Albany, Albany, NY 12222

FREDERICK SANDERS*

Center for Meteorology and Physical Oceanography, Massachusetts Institute of Technology, Cambridge, MA 02139

(Manuscript received 14 August 1985, in final form 2 December 1985)

ABSTRACT

A large-amplitude singular gravity wave is studied through the analysis of hourly observations, radar and satellite data and observations of cloud to ground lightning flashes. The wave activity was initiated just ahead of, and to the left of the track of, the major Atlantic Coast cyclone of 11–12 February 1983.

The initial wave of depression was followed by a wave of elevation and finally a wake depression. Pressure amplitudes were several millibars. The system propagated northeastward at 15 m s^{-1} accelerating to more than 25 m s^{-1} against increasing northeasterly flow in the lower troposphere.

Surface northeasterlies increased and became gusty with the approach of the first pressure falls, reaching a maximum at the pressure trough, then abruptly weakening and backing as strong pressure increases were observed. Strong fluctuations in column total condensation rate and radar reflectivity occurred with the passage of the wave.

Clustered lightning activity accompanied wave passage, principally near the intersection of the gravity wave and the east–west oriented escarpment of deep, high cloud along the north edge of the dry intrusion. A unique aspect was that lightning from clouds with relatively warm tops in the northern periphery of the dry intrusion lowered primarily positive charge to ground.

Disorganized wave activity developed in the presence of modest midtropospheric convection and beneath a shear zone in advance of a propagating jet streak. The singular appearing large amplitude wave organized subsequently in a transient zone of strong frontogenetical forcing. The wave appeared as the northern extension of a coastal front.

Overall, the system represented a ducted gravity wave propagating in a layer of large stability beneath an elevated layer of small Richardson number containing a critical level. Whether the accompanying convection and enhancement of condensation heating represented a forcing effect on the wave is unknown.

1. Introduction

Bandedness of the cloud and precipitation in the megalopolitan snowstorm of 11–12 February 1983 has been attributed by Sanders and Bosart (1985a,b) to frontogenetical forcing in the presence of small or negative symmetric stability. The linear structure was approximately parallel to the tropospheric thermal wind. Another striking aspect of the storm was a line of hourly-scale pressure oscillations of large amplitude, oriented approximately normal to the thermal wind. This singular perturbation was similar in strength and longevity to pulses described by Brunk (1949), Pothecary (1954), Wagner (1962), Ferguson (1967), Bosart and Cussen (1973), Eom (1975) and Pecnick and Young (1984). Like these examples, it displayed the character of a gravity wave. Unlike them, it was embedded in a region of continuous heavy precipitation and was directly associated with thunderstorms during its period of peak strength.

We present here a detailed analysis of the event based principally on routine hourly surface observations and on cloud-to-ground lightning flash data recorded by the East Coast lightning-detection network operated by the State University of New York at Albany (SUNYA), as described by Orville et al. (1983). The relationship of this oscillation to other observations of gravity-wave activity and to relevant theory is considered.

2. Synoptic circumstances

To supplement the account of the large-scale patterns provided by Sanders and Bosart (1985a), we show in Fig. 1 a conventional surface analysis over the eastern United States at the time the gravity wave was becoming organized. The prominent cyclone on the North Carolina coast was moving north-northeastward with

* Present address: Marblehead, MA 01945.

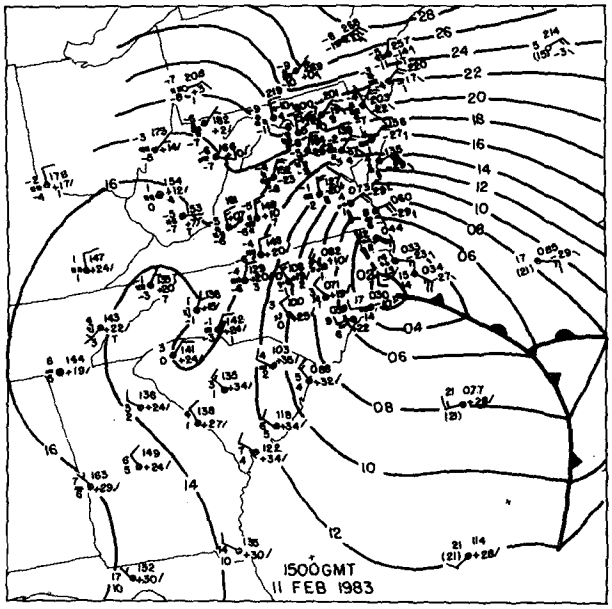

FIG. 1. Sea level isobars (solid, every 2 mb), pressure centers, surface fronts (conventional notation), station model [conventional notation with temperature and dew-point temperature in °C and 3 h accumulated precipitation (mm) where available] for 15 GMT 11 February 1983. Plotted winds in m s^{-1} with each full (half) barb denoting 5 m s^{-1} (2.5 m s^{-1}).

little change. Frontogenesis was evident northward from the low center into southeastern Virginia. An extensive shield of precipitation, much of it moderate or heavy snow, extended some 600 km north of the center. Aloft the flow was southwesterly. (The locations of places named or indicated by three letter designation in this paper appear in Fig. A1 of the Appendix.)

3. Oscillations of pressure

A series of maps of one-hour change of altimeter setting (station pressure reduced to sea level on the basis of standard-atmosphere temperature structure) appears in Fig. 2 for the period from 12 GMT 11 February until 08 GMT on the 12th (Synoptic Times in 2-digit hours). On the larger scale, pressure falls in advance of the low center occupy the southern half of the map initially. They move northeastward, dominating most of the area most of the time, to a final position in the eastern part, as broadscale rises advance from the southwest.

Superposed structures of smaller scale are abundant. Some of them show considerable temporal coherence as they emanate from the region of heavy snow around Maryland; for example, a weak surge of rises is seen near EWR in Fig. 2(d). Over the ensuing 5 h it propagates northeastward from this origin near the northern edge of the precipitation shield to New Hampshire and beyond, at speeds increasing from 20 to near 50 m s^{-1} [Fig. 2(i)]. It is not associated with precipitation, does not amplify, and is of little account.

Not so the feature which emerges at about the same time from Virginia. A mesoscale area of sharp falls followed by modest rises is apparent in Fig. 2(d), while a trailing area of falls makes its first appearance three hours later [Fig. 2(g)]. A concentrated area of lightning flashes is then observed in or close to the rise center as it intensifies and moves eastward toward Delaware. The electrical activity continues for the next three hours before rising to a crescendo (still modest by summer standards), accompanied by maximum amplitude of the rises in the period from 23 to 00 GMT, shown in Fig. 2(l). Thereafter, all the pressure change areas become more diffuse in turn, the leading falls losing their identity in the region of general falls over the Gulf of Maine (relatively sparsely observed by buoys), the rises accelerating northeastward across the same water and outrunning the snow area, and the following falls becoming impossible to identify after 06 GMT.

Some quantitative characteristics of the pressure oscillation and of the accompanying electrical activity are displayed in an illuminating manner in Fig. 3. The double amplitude, $2(\Delta p)'$, of the wave containing the leading fall center (A) was estimated by subtracting the greatest observed one-hour fall from the average of the two nearest maximum rises at stations (or minimum falls) along a general southwest–northeast direction. Similarly for the rise center (B), with maximum and minimum reversed of course, and for the trailing fall center (C). The wave length, L, was taken as the distance between the locations of the two flanking extremes. Small irregularities in the times series of $2(\Delta p)'$ and L arise from the necessity of using discrete station values. Lightning occurrences were counted within each half-hour period.

On first identification, the pressure waves show a double amplitude of 2–3 mb h^{-1} and horizontal scale about 200 km. Since the falls A precede the rises B, and the two are of equal magnitude, the wave appears first as a "hole" in the atmosphere, as in some of the cases cited, notably that of Pecnick and Young (1984). The scale of the oscillation shrinks to about 100 km 2–4 h after initiation, then slowly grows to nearly 500 km by the end of the observation period 12 h later. The double amplitude of the rise increases markedly with the onset of electrical activity, the peak of the rises reaching 8 mb h^{-1} at the time of maximum strike frequency. The system then appears more like a typical "thunderstorm high." Then both subside, the rises more abruptly than the lightning. Meanwhile the flanking falls intensify more slowly to double amplitudes of almost 6 mb h^{-1}, C becoming more prominent than A after 00 GMT, as the residual electrical activity becomes associated with it.

Various measures of the velocity of the disturbance can be obtained from Fig. 2, once the pressure features have become unambiguously established. The rise center, for example, moves toward 050–060 deg, at 15 m s^{-1} between 16 and 00 GMT, then accelerates to 24

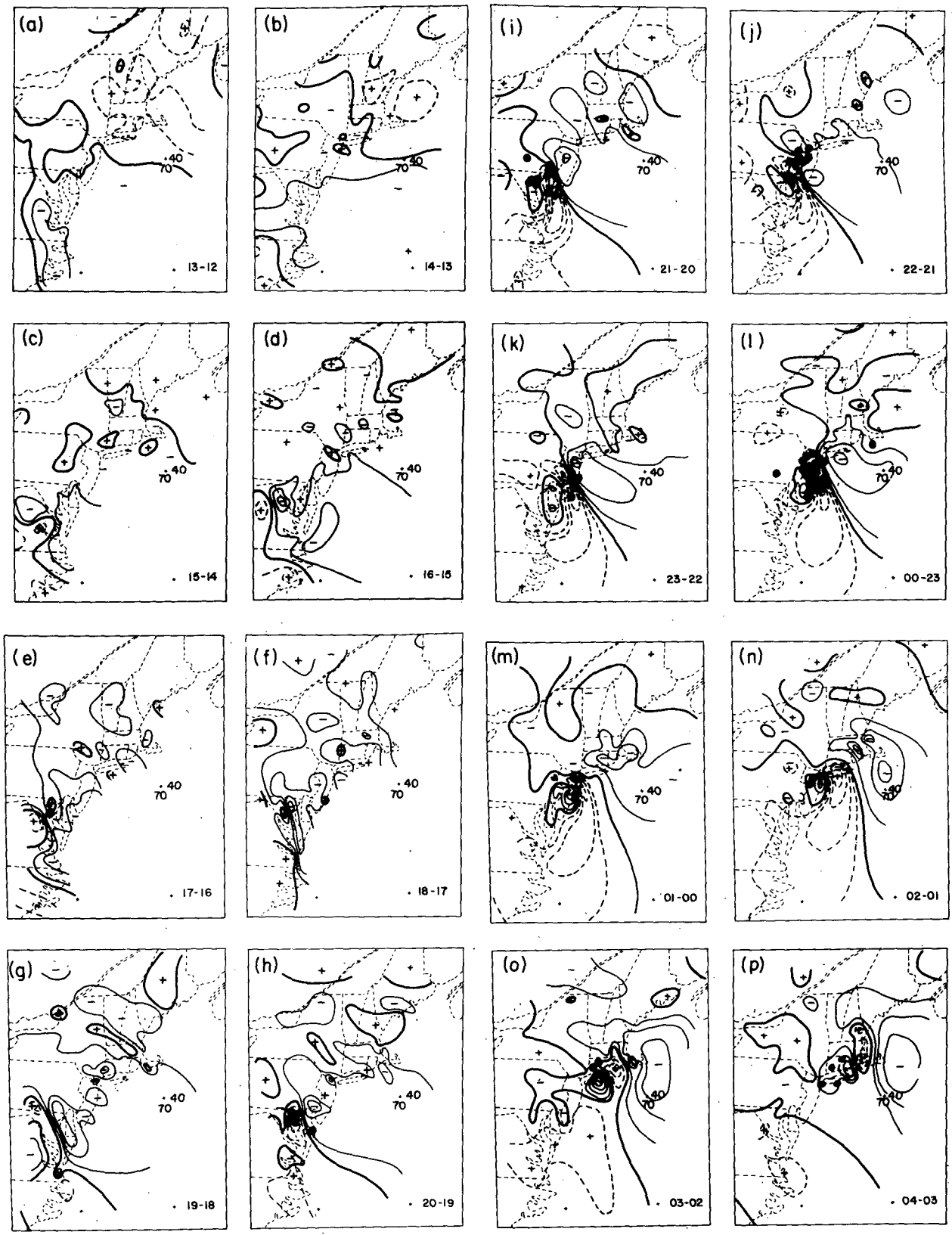

FIG. 2. Isopleths of hourly surface pressure change for the period 12 GMT 11 February through 08 GMT 12 February 1983. Falls (rises) denoted by solid (dashed) lines. Contour interval is 1 mb with the zero contour a heavy solid line. Solid circles denote lightning locations from the SUNYA lightning detection network for the hour ending at each map time. Figure is arranged in groups of 4 maps. Time difference (GMT) is indicated in the lower right corner of each figure panel. Time (a) corresponds to the hour ending 13 GMT 11 February; time (t) to the hour ending 08 GMT 12 February.

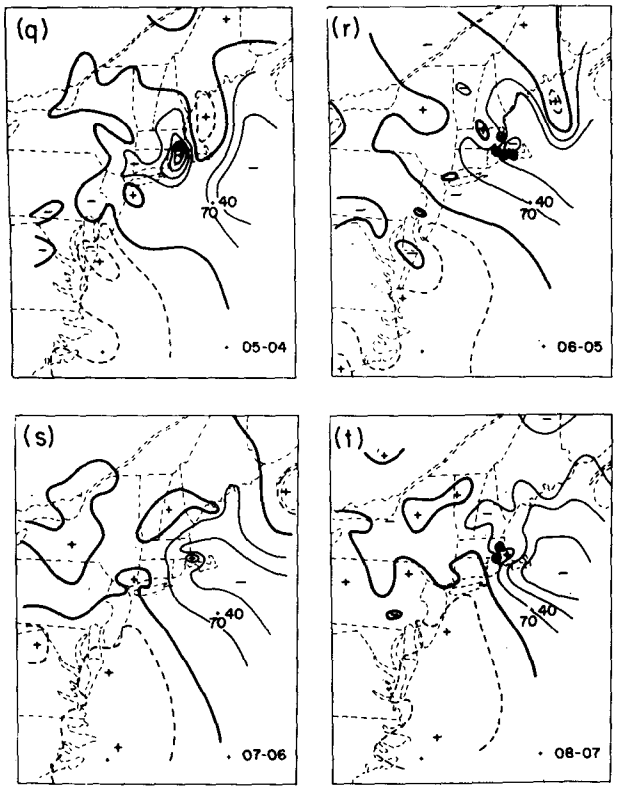

FIG. 2. (*Continued*)

m s^{-1} in the next 4 h and to 42 m s^{-1} from 04–07 GMT, as it moves out away from the snow area. This behavior is similar to that shown by the earlier area of weak rises. The leading fall center moves at 15 m s^{-1} between 15 and 21 GMT, accelerating to an average speed of 22 m s^{-1} over the next 5 h prior to losing its identity. The trailing center moves at 17 m s^{-1} between 19 and 02 GMT before accelerating to 23 m s^{-1} from that time until 06 GMT. All three components of the system thus start out at a speed of about 15 m s^{-1} and accelerate to more than 20 m s^{-1} after a few hours.

Since the system as a whole accelerates as its scale increases, its frequency changes relatively little. Consider the early, middle and late portions of the period of main interest to be 16–20 GMT, 20–24 GMT, and 00–04 GMT, with associated system speeds (from Fig. 2) of 15, 17 and 23 m s^{-1} and wavelengths (from Fig. 3) of 130, 170 and 280 km. Then the period of the system increases from an early value of 2.4 h to a middle one of 2.8 h and finally 3.4 h.

We must acknowledge that truncation error is severe in analyzing this system with data at intervals of one hour, a point emphasized by Stobie et al. (1983). On occasions when the peak changes were occurring between stations it was necessary to guess creatively. Hence much of the irregularity in Fig. 3.

4. Effects on weather elements

a. Wind

The influence of this gravity wave on the weather elements can be inferred from the idealized vertical cross section after Eom (1975), shown in Fig. 4. (The vector difference between the gravity wave phase velocity and the basic current determines the dynamics of gravity wave behavior. Omission of the basic current in the simple model shown in Fig. 4 is permissible here because the wave is propagating rapidly against the basic flow which allows for the rapid transit time of an individual air parcel through the gravity wave disturbance. For a gravity wave propagating slower than the basic current the attendant vertical motions, pressure falls and wind perturbations shown in Fig. 4 would be reversed.) As the low-pressure trough approaches, in the model, the wind increases from the direction toward which the wave is propagating. In the present case, the wave is traveling toward the northeast, against a substantial northeasterly basic current, which must be

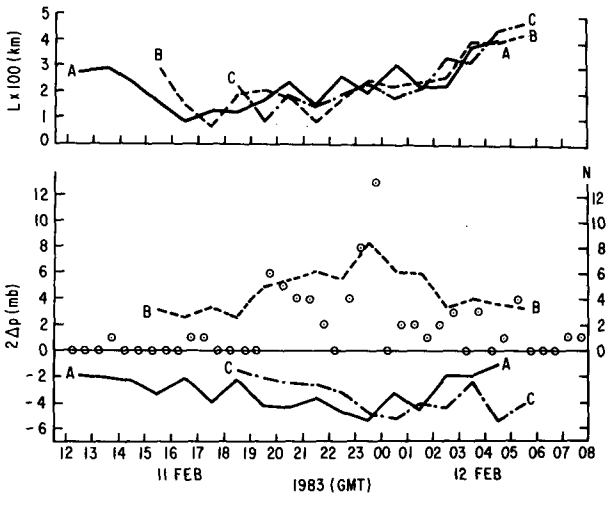

FIG. 3. Time series of the wave length, L (top), and the double amplitude, $2(\Delta p)'$ (bottom), for the region B centered on the rises (dashed lines) and of the regions A (solid lines) and C (dash-dot lines) centered on the leading and trailing falls, respectively. See text. The circled dots indicate the number of lightning flashes detected by the SUNYA system each half-hour.

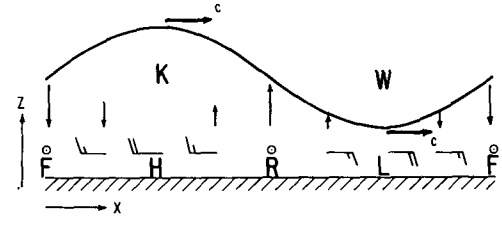

FIG. 4. Idealized vertical cross section of a linear plane gravity wave, with no basic current, propagating toward the right at speed, c. The heavy sinusoidal line is a representative isentropic surface or a temperature inversion. Surface pressure extrema are labeled H and L, while cold and warm temperature anomalies are denoted K and W, respectively.

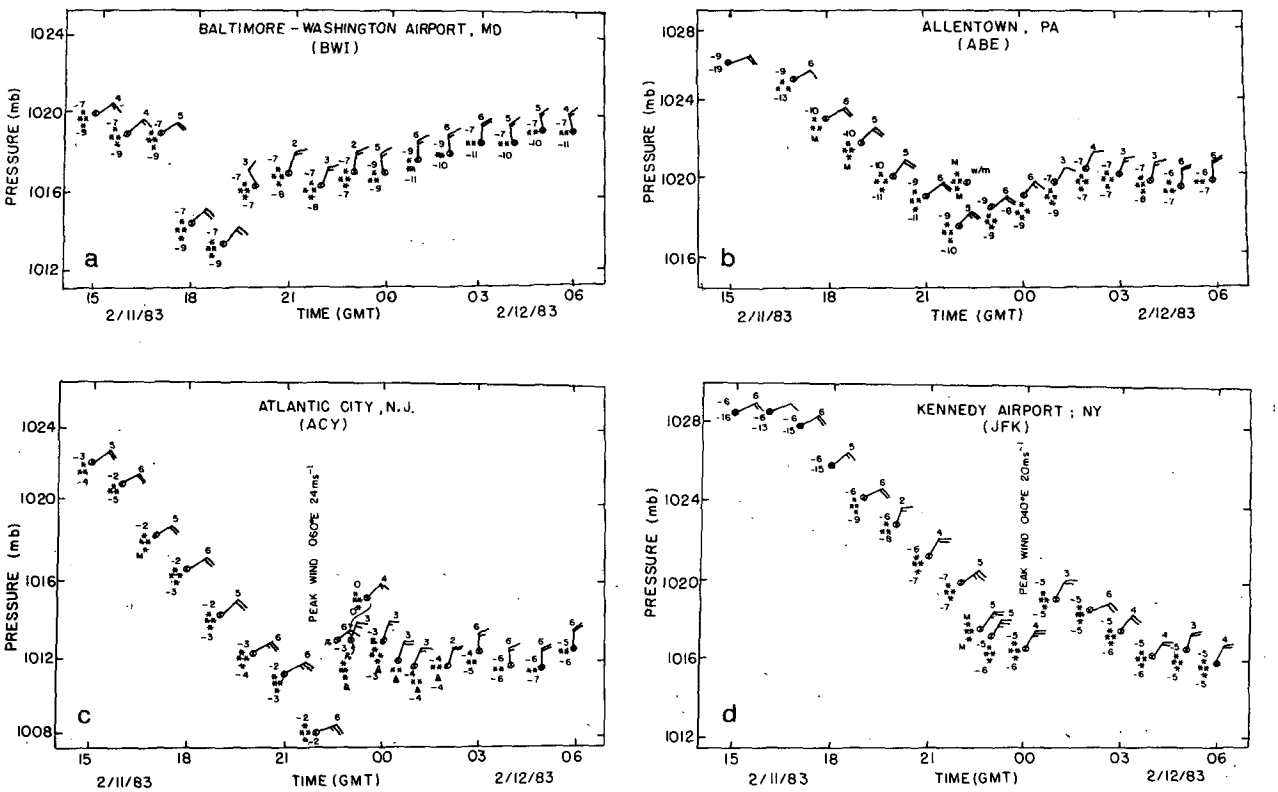

FIG. 5. Time section of hourly and special observations as a function of mean sea level pressure (mb) (a) for BWI; (b) for ABE; (c) for ACY; (d) for JFK. Plotting model as in Fig. 1.

added to the model. The northeasterly wind should therefore increase to maximum strength at the time of lowest pressure. As examples of actual data, we present time series of surface observations from four stations in Fig. 5; recorder traces of pressure and wind at College Park, Maryland (CPK)[1] are shown in Fig. 6. This effect is seen at CPK and at all stations in Fig. 5. Similar gusty easterly winds were reported in the cases studied by Brunk (1949), Ferguson (1967) and Bosart and Cussen (1973).

Almost all stations affected by the wave show a response attributable to the intense pressure gradient associated with the rapid pressure rise. Southwesterly winds, as suggested by Fig. 4, are not observed; rather, owing to the strong basic current, the northeasterlies weaken and back, as far as northwest in some instances (cf. BWI in Fig. 5 and CPK in Fig. 6). A map of this one-hour vector shift is presented in Fig. 7. The direction of the change is southwesterly, for the most part, with magnitude undergoing an evolution like that of the pressure amplitude shown in Fig. 3, except that the strongest wind shifts occur between 20 and 22 GMT,

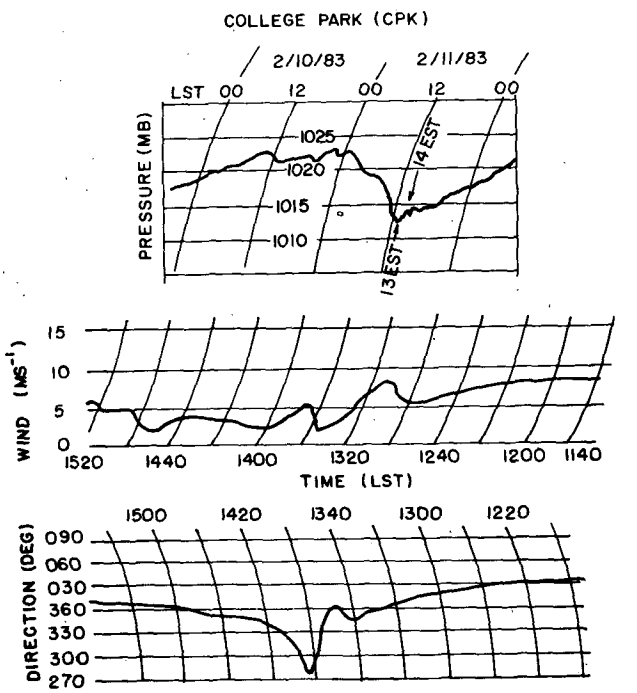

FIG. 6. Detailed data for College Park, Maryland (CPK). Barogram at top and wind speed and direction at center and bottom, respectively.

[1] The barogram was kindly provided by Dr. R. C. Taylor and the wind traces by the University of Maryland.

2–3 h earlier than the greatest pressure rises (compare curve B in the lower panel of Fig. 3). The positions of the maximum hourly wind shift match closely those of the maximum hourly rise. In view of the periodicity, the end of the hour of maximum change is usually approximately the time of extreme value. Thus Fig. 4 is confirmed.

The consistency of the analysis can be given a rough check by application of Gossard and Munk's (1954) "polarization relationship," from which we can obtain

$$v' = \frac{p'RT_0}{p_0(c-u)} \tag{1}$$

where v' can be identified with half the wind shift shown in Fig. 7, and p' with half $2(\Delta p)'$ in Fig. 3 and u is the speed of the basic current. Then for the early, middle, and late periods delineated in the preceding section, p' is taken as 2, 3, and 2 mb, and c (as before) as 15, 17, and 23 m s^{-1}. With p_0 = 1015 mb, T_0 = 270 K, and u = −7 m s^{-1}, we obtain v' values of 7, 10, and 5 m s^{-1} for the three periods, respectively. Inspection of Fig. 7 shows that these values are 10–20% too large. It is likely that surface friction damps the wind response to the wave. The variability of this damping as well as variation in the pressure structure (and perhaps truncation error), accounts for the station-to-station differences in Fig. 7. With this qualification, the consistency of the analyses is supported by the polarization relationship.

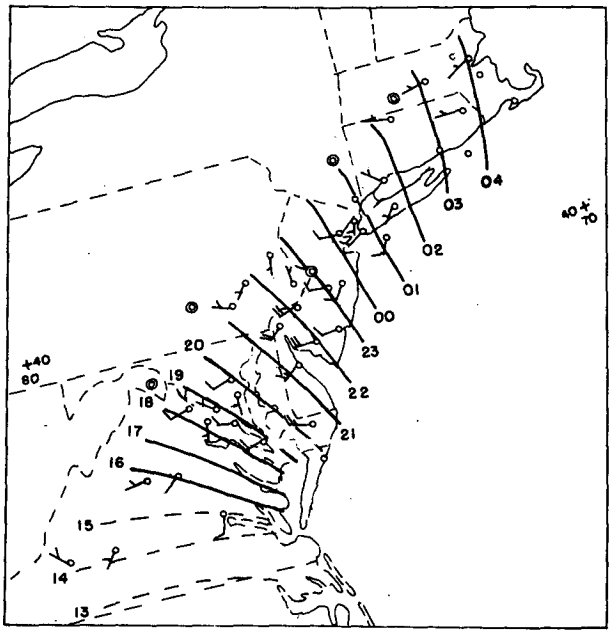

FIG. 7. Isochrones of the time (GMT) at the end of the hour of greatest vector wind shift. Dashed line indicates the ill-organized phase. One full (half) represents 5 m s^{-1} (2.5 m s^{-1}) magnitude of vector shift.

b. Cloud and precipitation

The descent and adiabatic warming in the region of pressure fall should tend to discourage precipitation and dissipate cloud. Brunk (1949) notes diminished thunderstorm activity at the time of lowest pressure in his case study, with largest pressure amplitude in a region of little or no rain. In Ferguson's (1967) case, the data shows a cessation of precipitation during the time of rapidly falling pressure and strong northeasterly wind, while Bosart and Cussen (1973) show an end of precipitation as the trough of low pressure passes.

Conversely, ascent occurs in the region of pressure rise in Fig. 4, and in the aforementioned instances, as in Pothecary's (1954) case, there was evidently a resumption of precipitation or development of cloud. A similar phenomenon was noted by Uccellini (1975).

In the present case the entire system is embedded in a heavy snowstorm, so that the vertical displacement due to the wave is superposed on substantial ascent of larger scale, as shown by Sanders and Bosart (1985a). It is not possible to infer anything systematically from the hourly observations of snow intensity because, as seen in Fig. 5, it is heavy throughout. For every supportive change in visibility there is a contradictory one. Perhaps this is to be expected given the dilatory fall velocities of crystals, the strong winds at low levels, and the difficulty in distinguishing between falling and blowing snow.

Direct MIT Doppler radar evidence of the effect of the wave was presented, however, by Sanders and Bosart (1985b). The leading fall area could not be detected clearly on radar in the MIT area, as this feature was propagating out of the precipitation shield at the time. The enhancement of updraft with the passage of the rise area is clearly shown around 03–04 GMT in their Fig. 3b, as is suppression of ascent 2 h later as the trailing falls moved by. The integrated condensation rate dropped by a factor of 2.4 during this episode. The snowfall rate at the ground during the storm was reported as heavy only in the two hours following the wave-enhanced ascent, but equally low visibility was recorded at other times, due to a mixture of blowing and falling snow. There was no report of enhanced snow accumulation on the ground that could be attributed to the wave. Thus it seems that the undeniable effect of the wave on overhead condensation rate is not clearly related to ground accumulation, owing to complexity of physical process and to difficulty of observation. [Uccellini (personal communication, 1985) observed at least three distinct bursts of snowfall at a point between DCA and BWI so the difficulty of determining precipitation rates must not be underestimated.]

Further radar evidence of an impact of the wave on weather phenomena is seen in the radar reflectivity data. In the manually digitized radar (MDR) maps for NHK (Fig. 8) we see modest echoes at 1735 GMT just

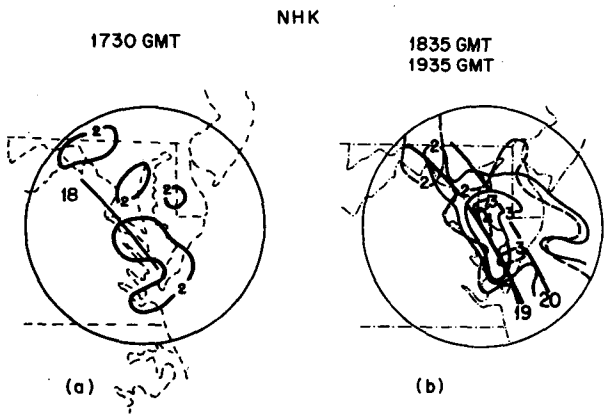

FIG. 8. Manually digitized radar (MDR) intensity contours for the National Weather Service WSR-57 radar at NHK for the time indicated. Precipitation intensity code 2 rainfall rates from 2.5 mm h^{-1} if weak and stratiform to 28 mm h^{-1} if convective and heavy. Code 3 ranges similarly from 12.5 to 56 mm h^{-1}, while Code 4 denotes convective precipitation in the range from 56 to 114 mm h^{-1}. Appropriate wind-shift isochrones from Fig. 7 are superposed. (a) 1730 GMT and (b) 1835 GMT (dashed) and 1935 GMT (solid).

ahead of the strong wind shift. (Bear in mind that the 18 GMT one-hour wind-shift isochrone can be taken to represent the instantaneous shear of the wind at 1730 GMT.) These echoes move relatively little, lying just behind the strengthening wind shift and pressure rise two hours later. The first group of lightning flashes are just beginning at 1935 GMT in the northern portion of the strong-echo region. No useful radar observations were available at NHK after 1935 GMT or between NHK and MIT, where Sanders and Bosart (1985b) showed that the rises enhance and the falls then temporarily fragment a pronounced band of high reflectivity due to a frontal circulation as the wave system moves through it.

Detailed satellite imagery is informative. The 4-km infrared information for 21 GMT (Fig. 9a) indicates a pronounced drop in cloud top from north to south along a line across northern Delaware, southern New Jersey and southeastward. We see a prominent double intrusion of moderately high tops into the low-top region near the propagating surface wind shift. This is clearly associated with the gravity wave. The leading intrusion overlies the pressure trough, while the following stronger one lies near the rapid rise.

The 1-km visible imagery for 30 minutes later is shown in Fig. 9b. The high clouds to the north appear quite amorphous, while in the lower clouds there are many bands, 10–20 km apart and 5 km apart over the ocean east of Delaware and over Virginia, respectively. The orientation of these bands is evidently more or less parallel to winds in the lower troposphere. The surface wind-shift line, at a large angle to the bands, enhances them along the intersection running southward from southern New Jersey but does not disrupt them completely. We surmise that the radar echoes at 1935 GMT (Fig. 8) correspond to the cold intrusion in the satellite imagery at 21 GMT in Fig. 9a. Note the similarity in shape of the Code 3 intensity isopleth and the −25°C isotherm. Once formed in the pressure trough ahead of the growing rises (contrary to the indications in the idealized Fig. 4), the band of most intense cloud progresses northward with the wave, in accord with the idealized model.

A broader view of the impact of the wave on the higher cloudiness can be obtained from Fig. 10. Since the winds in the upper troposphere are strong southwesterlies, the appearance of cold tops in southern New Jersey at 20 GMT (Fig. 10d) and in southern New England at 02 GMT (Fig. 10f) represent growth attributable to the wave, rather than translation of existing cloud. Similar evidence is provided by Sanders and Bosart (1985b). The wave propagates entirely through the high cloud shield, however, and its effect is not dramatic.

Mention should also be made that the heavy snow region in Fig. 10, which initially lies near the southern edge of the highest and coldest cloud, is gradually left behind by the faster moving cold cloud mass. This is entirely consistent with the idea of a sloping synoptic scale updraft in middle latitude cyclones as has been documented by numerous investigators (e.g., see Bjerknes, 1919; Green et al., 1966; Carlson, 1980). We add that the embedded patchiness of the individual cloud top elements is a manifestation of smaller scale processes in the storm dynamics. We note without further comment that quantitative precipitation forecast schemes based primarily upon cloud temperature characteristics will fail miserably in these situations.

c. *The thunderstorms*

A striking effect produced by the wave was the electrical activity discussed above in relation to the pressure oscillations. Thunder was reported at numerous surface stations, as shown in Fig. 11. The exact times of the period of thunder could not be determined in many instances but the isochrones in Fig. 11 are consistent with all available information. It is seen that they are consistent with the SUNYA observations (Fig. 2) and are approximately synchronous with the surface wind-shift depicted in Fig. 7.

The actual lightning locations are shown in Fig. 12. Positive polarity is indicated along with the time of the surface wind shift as it passed through each lightning cluster. It seems significant that all the SUNYA ground-flash observations (except an early one unrelated to the gravity wave) occur over land or within 25 km of the coast. Close examination shows that about 60% of the 69 flashes are clustered in one of four more-or-less discrete episodes, initiated at 1931 GMT between DCA and BWI [Fig. 2(g)], at 2248 GMT just northeast of ACY [Fig. 2(l)], in southwestern to central Connecticut at 0219 GMT [Fig. 2(o)], and between PVD and BOS at 0456 GMT [Fig. 2(r)]. Another half-dozen flashes are grouped in the New York City area starting about

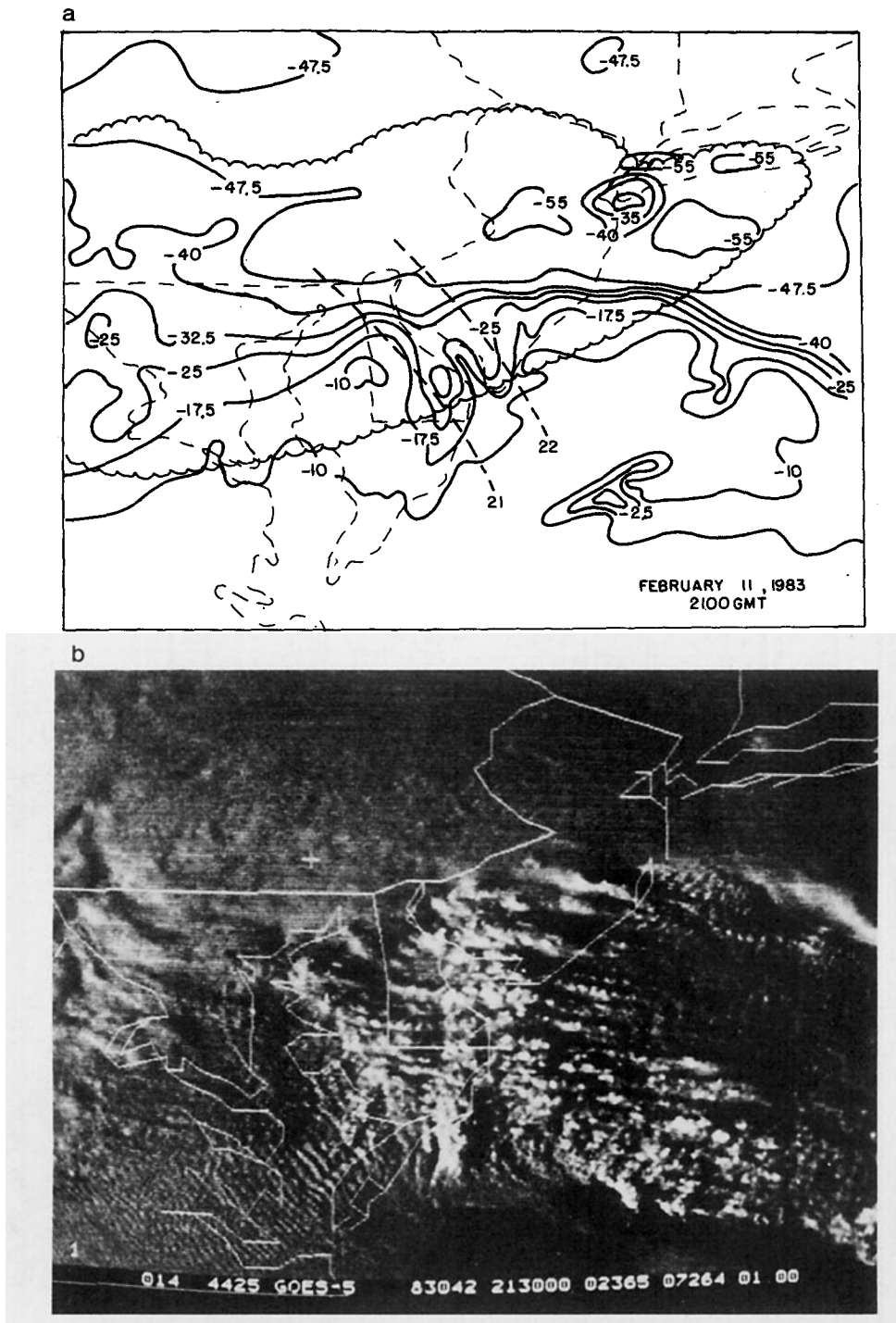

FIG. 9 (a) Cloud top temperature (°C) analysis at 21 GMT 11 February 1983 from 4 km resolution infrared satellite image available on the SUNYA McIDAS system. Simultaneous isochrones of the surface wind shift are transcribed from Fig. 7. Scalloped line outlines region of continuous moderate and heavy precipitation. (b) McIDAS 1 km visible satellite image for 2130 GMT 11 February 1983.

2332 GMT [Fig. 2(m)]. All of these clusters, except perhaps the one in east-central New Jersey, occur along or near the south edge of the deep cloud area, where it is intersected by the surface windshift line. The exception occurs in the zone of cloud buildup to the south, but the thunderstorms are also along the windshift line.

Each localized region of electrical activity tends to remain in place for a few hours rather than move with the winds aloft or propagate with the gravity wave. In

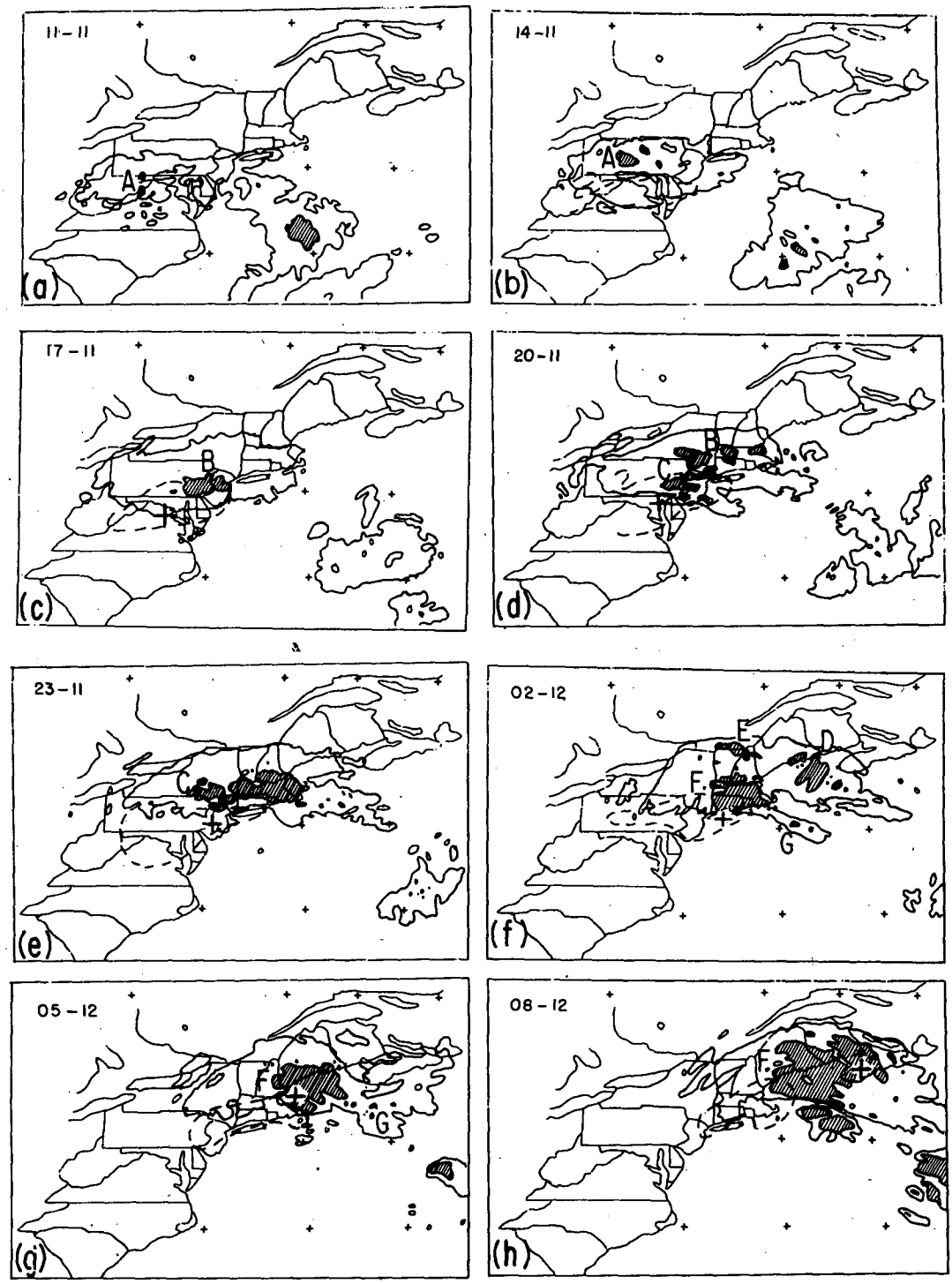

FIG. 10. Outlines of areas of cloud-top temperatures lower than −53°C (shaded) and −42°C (not shaded) as estimated from GOES satellite infrared imagery, 3 h intervals (a) beginning 11 GMT 11 February 1983 and (h) ending 08 GMT 12 February 1983. Area of moderate or heavy snow enclosed by dashed line. Letters denote discrete areas of cold cloud. Plus sign indicates position of maximum one-hour pressure rise, ending at hour of map, for high amplitude gravity wave.

the areas described above, the last flashes occur at 2305 GMT, at 0105 GMT, at 0334 GMT, at 0733 GMT and at 0352 GMT, respectively, as can be confirmed by examination of the appropriate panels in Fig. 2. Thus, these thundery groups, once triggered, appear more fastened to something on the earth's surface than to something in the atmosphere.

The exceptional southward-extending thunderstorm

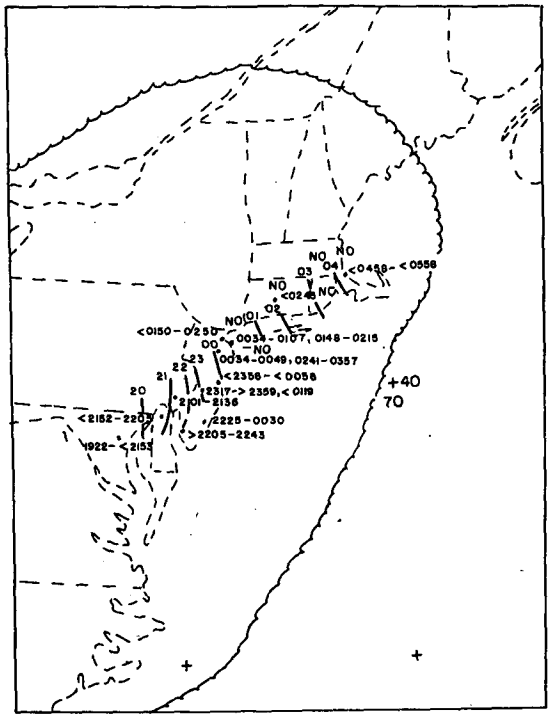

FIG. 11. Beginning and ending times (GMT) for thunderstorms at hourly reporting stations 11–12 February 1983. A "NO" indicates that thunderstorms were not reported at that location. Isochrones of start of thunder given by short line segments (see Fig. 7 for more complete information on gravity wave). Inequalities indicate inability to determine the precise time of beginning or ending of thunder. Scalloped line outlines region of likely ground flash detection.

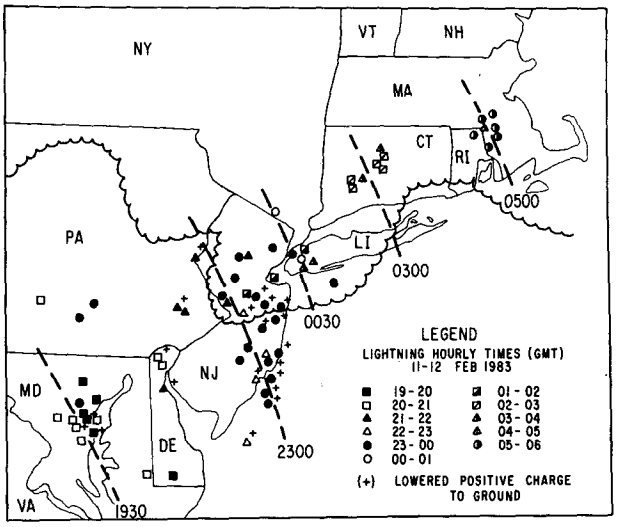

FIG. 12. Lightning locations from the SUNYA network for the period 18 GMT 11 February through 06 GMT 12 February 1983. Hourly time sequence according to legend. Appropriate wind shift lines from Fig. 7 are superimposed. Scalloped line encloses region of continuous cloud top temperatures < −32°C at 00 GMT 12 February 1983.

outbreak in New Jersey is distinctive also in that all flashes south of the northernmost ones carry positive charge to the ground, whereas all subsequent flashes to the north and east lower negative charge. What is unusual about these storms?

The nominal 00 GMT sounding from ACY appears in Fig. 13. The balloon was probably released shortly after 23 GMT, just after the start of the thunderstorm activity and on its southwest edge, but thunder is heard at the station at 23 and 00 GMT. There is little instability for upright convection, with potential instability indicated only for the layer between 680 and 500 mb. The cloud top is indicated at 590 mb at a temperature of −14°C, consistent with the cloud-top temperatures in Fig. 9a in the region south of the deep cloud. Now if the unsaturated air at 540 mb were raised by the gravity wave to its lifting condensation pressure and temperature of 460 mb and −30°C, then air rising in an undilute cumulus updraft from 680 mb would have 2°C of buoyancy at this level but would be unable to penetrate much farther, owing to the stability of the ambient atmosphere above.

Thus the thunder-producing cumulonimbus would be weak examples with tops warmer than those of most thunderstorms consistent, however, with the cloud-top temperatures indicated in Figs. 9(a) and 10(e). The available evidence, therefore, suggests that these relatively mild, shallow thunderstorms lower positive charge to the ground. A substantial fraction of thunderstorms southwest of ACY lower positive charge as well, but Fig. 10 and Fig. 12 (coldest tops tend to be north of the region where positive charge is lowered to ground) and data presented by Sanders and Bosart

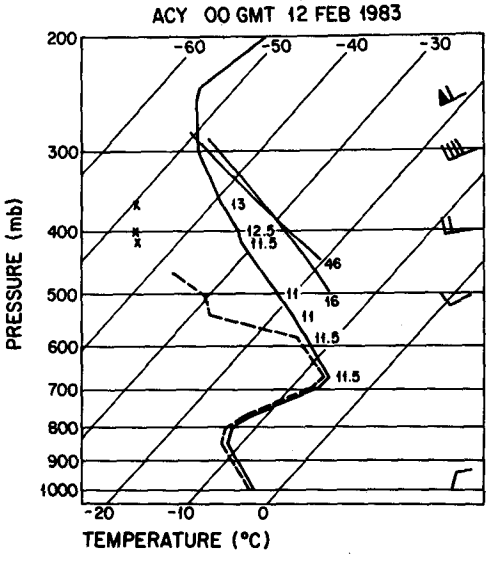

FIG. 13. Sounding from ACY 00 GMT 12 February. Temperature and dew point shown by solid and dashed lines, respectively. Plotted values denote wet-bulb potential temperature (°C). Thin lines represent 46°C dry adiabat and moist adiabat for 16°C wet-bulb potential temperature. Partial winds for IAD (ACY wind equipment failed) with pennant, full barb and half barb denoting 25, 5 and 2.5 m s^{-1}, respectively.

(1985b), suggest that these, but not those northeast of the New Jersey outbreak, may be shallow. Even the latter, however, are likely weak, to judge from the instability of the ambient atmosphere, so it seems that cloud-top temperature, rather than updraft vigor, may determine the electrical character, if we may hazard a frail conjecture. The question is of practical as well as scientific interest, because of the potential disruption of power grids and transmission facilities by positive flashes which tend to exhibit higher peak currents than negative flashes (Brook et al., 1982).

Takeuti et al. (1978) and Brook et al. (1982) have reported that winter thunderstorms along the Hokuriku coast of Japan often lower positive charge to ground. Brook et al. (1982) noted a strong correlation between the fraction of positive ground flashes and the vertical shear in the cloud layer. They reasoned that the presence of a sheared environment enabled positive streamers from the upper region of the cloud to reach the surface rather than the negatively charged regions in the lower part of the cloud as would be the case in an unsheared environment. They suggested a shear threshold of 1.5 m s^{-1}/km for the appearance of positive strokes to ground. While the absence of wind information at ACY (Fig. 13) precludes a determination of the actual shear in the present case the results of Sanders and Bosart (1985a) indicate that the geostrophic shear is well above this threshold.

An alternative explanation of the electrification might appeal to the updrafts, and especially the strong shears, in the frontal circulation or perhaps in "slantwise convection" resulting from symmetric instability, which were evidently present in this storm. If this were the agent, however, the clusters of activity would have occurred randomly along the baroclinic zone, rather than in close relation to the gravity wave, as observed.

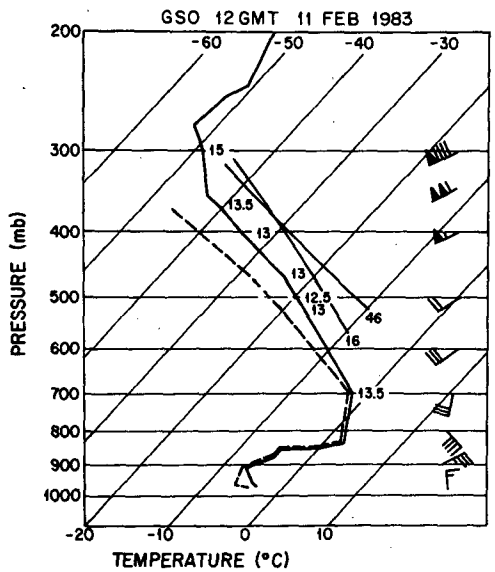

FIG. 14. As in Fig. 13 except for GSO at 12 GMT 11 February 1983.

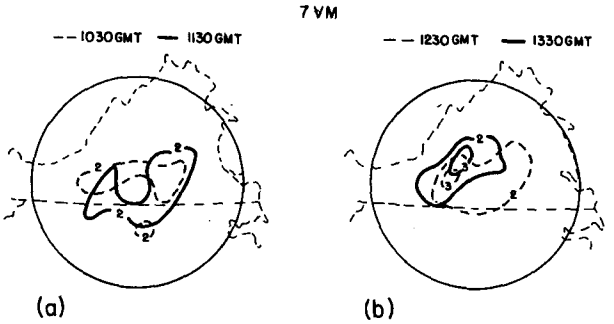

FIG. 15. As in Fig. 8 except for 7VM at times indicated.

5. The origin of the wave activity

In the present case, the wave activity that leads to the development of the large-amplitude oscillation originates northwest of the surface low center in the Virginia–North Carolina region shortly after 12 GMT (cf. Figs. 1, 2a–c). The nearest available sounding, from GSO at 12 GMT (Fig. 14), shows a structure similar to that of ACY 12 h later (Fig. 13), except that the potentially unstable layer is deeper (700–400 mb) and the wet-bulb potential temperature in the layer is about 2°C higher. Modest convective clouds develop up to near 360 mb with little modification of the sounding by the frontal circulation presumably present. The cloud-top temperatures would be near −40°C, and in fact the satellite infrared imagery in Fig. 10(a) shows a number of small cloud elements of about this temperature downwind (aloft) from GSO, moving north to merge with the main cloud mass.

Radar observations from 7VM around this time, shown in Fig. 15, support this view. Echoes of intensity code 2, or 3 (superposed on a broad coverage of code 1, not shown) are present over a 3-h period during which the observer annotations indicate the likelihood of thunder with numerous cloud tops at 7.6 km. This elevation is just above the 400 mb level in good agreement with indications from the GSO sounding. A maximum radar top at 9.8 km is evidently produced by an air column with somewhat greater instability than indicated at GSO. There are no observations of lightning in this region from the SUNYA network, and no reports of lightning or thunder from ground observers, but it seems likely that the first disorganized gravity wave activity was initiated by weak cumulus convection aloft above a deep layer of large stability, as seen in Figs. 13 and 14.

An alternative, or supplementary, possibility is suggested by an extraordinary wind shear in the GSO sounding, from 255 deg, 27 m s^{-1} at 400 mb to 250 deg, 54 m s^{-1} at 343 mb, over a depth of 1.1 km with nearly neutral stratification. (Given that the wave propagates toward the northeast at 15 m s^{-1} in its initial stages it is evident from the GSO sounding that a critical layer exists between 500 and 400 mb in the lower por-

tion of the strong shear region between 500 and 343 mb.) The near-zero Richardson Number there indicates the likelihood of shear-generated gravity waves, as observed in cases studied by Reed and Hardy (1972), Hooke and Hardy (1975) and Gedzelman and Donn (1979), among others. It appears, however, that these waves usually have amplitudes of the order of tenths of mb and periods of the order of ten minutes, an order of magnitude shorter and smaller than the oscillations examined here. Spatial and temporal coherence are evidently much smaller as well. Stobie et al. (1983), however, have provided evidence of long-lived shear-generated waves which are comparable in scale to our example. They, as well as Pecnick and Young (1984) associate the generation of these waves with the approach of a mobile synoptic-scale trough, with its intensified jet maximum. Such a scenario fits this case reasonably well. There is evidence in any event of high-frequency variations in this case, as close study of the barogram (e.g., Fig. 6) shows. Pothecary (1954) and Wagner (1962) commented on the presence of such shorter-period waves in their studies which were directed mainly at the larger phenomenon. Since warm unstable air and strong upper-tropospheric winds and shears occur together in this example, as in most, it is not impossible to attribute the origin of wave activity to a single source.

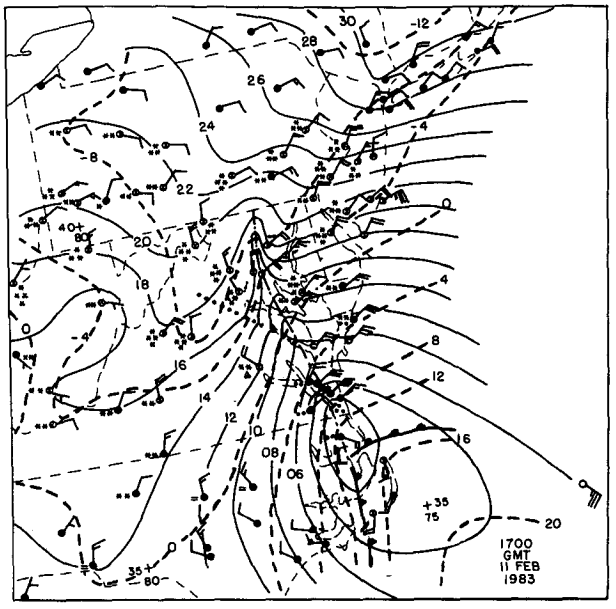

FIG. 16. As in Fig. 1 except for 17 GMT 11 February 1983.

6. Organization of the large-amplitude wave

Whatever the origin of the disorganized activity, the distinctive characteristic of the large-amplitude feature is its singularity. This aspect in other instances no doubt attracted the attention of the investigators cited in the Introduction, as it is a fairly rare event, analogous perhaps in some sense to the "rogue wave" at sea. Our New England experience confirms the statement by Pecnick and Young (1984) that this type of event occurs at a given Midwestern point about once per year. This singular aspect sets the present phenomenon apart from other gravity wave trains of similar amplitude, period and wave length (e.g., Uccellini, 1975; Miller and Sanders, 1980; Stobie et al., 1983) which are ultimately associated with widespread intense cumulus convection, as a sporadic prominent source of forcing and response.

It may not be coincidental that organization of the wave occurred near the time and location of intense surface frontogenesis. The calculation illustrated in Fig. 17 for the map given in Fig. 16 was carried out on an 0.5 degree latitude and longitude grid from the expression:

$$\frac{d}{dt}|\nabla T| = \frac{1}{2}|\nabla T|\left\{\left(\frac{\partial u}{\partial x} - \frac{\partial v}{\partial y}\right)\sec 2\alpha \cos 2\beta - \nabla \cdot \mathbf{V}\right\} \tag{2}$$

where u and v are the zonal and meridional components of the observed wind, α is the angle between the x-axis and the axis of dilatation of the deformation field, and β is the angle between the isotherm and this axis. The geostrophic deformation was evaluated from the pressure analysis according to Saucier (1955). The elongated pronounced maximum in the Chesapeake Bay area at 17 GMT in fields based on geostrophic as well as on actual winds corresponds closely, in time and location, to the organization of the strong singular wave (cf. Fig. 2e–g) prior to the onset of intense convection.

Ley and Peltier (1978) have shown, in the context of the model of frontogenesis presented by Hoskins and Bretherton (1972), that this process can emit a packet of gravity waves which propagates (albeit too slowly in the calculation discussed) out ahead of the developing front. In the present case, in which the frontogenetical aspects will be comprehensively reported later, the front growing northward from the center in Fig. 1 reaches only up to the southern portion of Chesapeake Bay. The gravity wave then appears to be northward extension of the front, its passage not accompanied by any significant temperature change (cf. Fig. 5).

7. Propagation speed and physical character of the wave

Calculation of the propagation speed of gravity waves from a formula or equation set is often used (e.g., Wagner, 1962; Bosart and Cussen, 1973; Eom, 1975; Lindzen and Tung, 1976; Stobie et al., 1983) as evidence for the appropriateness of the physical theory being applied. Results, ranging from 14 to about 50 m s^{-1}, are invariably satisfactory. A particularly simple

formula, representing the propagation speed, c, of a wave along an inversion at height h separating two unstratified air layers with potential temperature θ_1, below and θ_2 above has been widely used. It is

$$c_{\text{inv}} = \left[gh\left(\frac{\theta_2 - \theta_1}{\bar{\theta}}\right)\right]^{1/2}. \tag{3}$$

Lindzen and Tung (1976), for a more realistic structural model of a ducted gravity wave propagating in a stable layer of depth H with Brunt–Väisälä frequency $N = [(g/\bar{\theta})\partial\theta/\partial z]^{1/2}$, present (for the gravest vertical mode)

$$c_{\text{duct}} = \frac{NH}{\pi/2}. \tag{4}$$

If θ_1 and θ_2 are the potential temperatures at the bottom and top of the stable layer, this formula becomes

$$c_{\text{duct}} = \frac{1}{(\pi/2)}\left[\frac{gH(\theta_2 - \theta_1)}{\bar{\theta}}\right]^{1/2}, \tag{5}$$

which has a strong resemblance to (3).

Soundings along the path of the gravity wave, as pointed out by Sanders and Bosart (1985a), display a characteristic structure, as illustrated, for example, by GSO at 12 GMT 11 February and by ACY at 00 GMT 12 February (Figs. 14 and 13, respectively). In the former, a stable layer extends from a base at 905 mb (potential temperature θ = 274 K) to a top at 830 mb (θ = 291 K) with a depth of 700 m. If this structure were idealized by an inversion representing a discontinuity in θ, then its elevation might be taken as the middle of the stable layer, at 1300 m. For the latter sounding, θ ranges from 274 to 299 K over a stable layer 1800 m deep with a mean elevation of 2400 m.

In the GSO sounding (Fig. 14), notice that while the

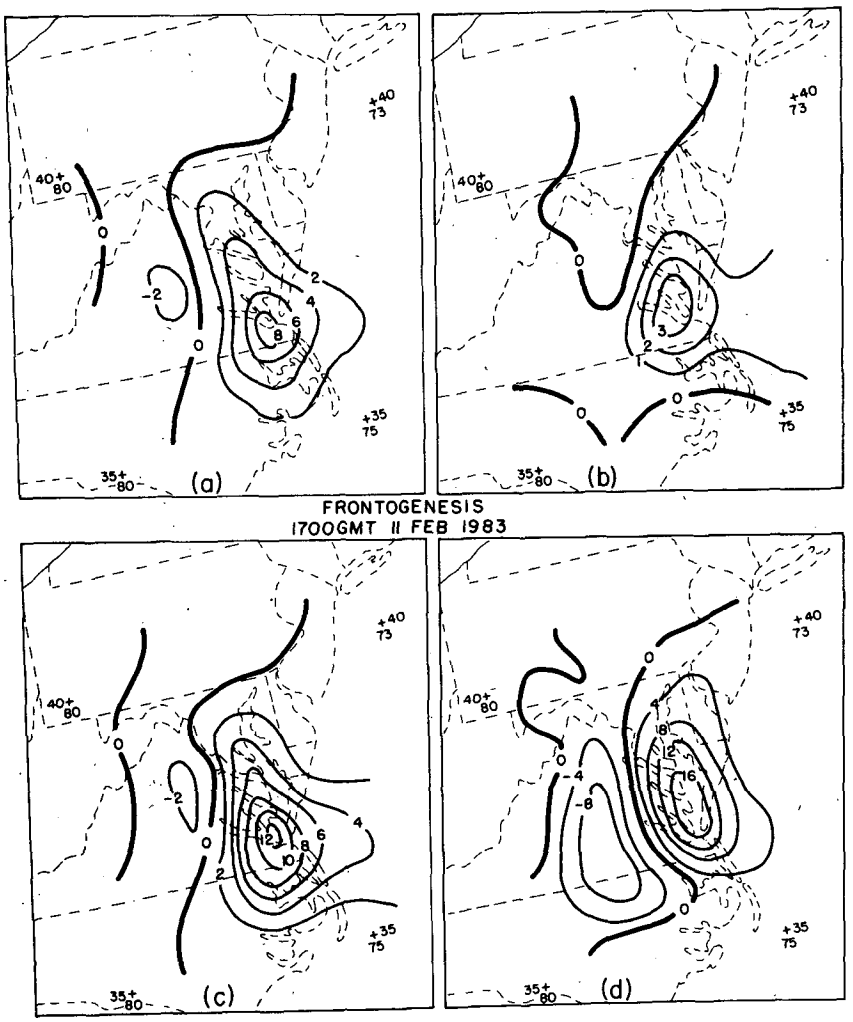

FIG. 17. (a) Divergent wind contribution to frontogenesis for 17 GMT 11 February 1983. Units: °C (100 km)$^{-1}$ (3 h)$^{-1}$. (b) As in Fig. (a) except for deformation contribution. (c) Total frontogenesis (Fig. 17a plus Fig. 17b) and (d) Geostrophic total frontogenesis for 17 GMT 11 February 1983. [Units: °C (100 km)$^{-1}$ (3 h)$^{-1}$].

base of the stable layer is unambiguously defined, the top is not. An alternative choice might be at 700 mb, at the base of the nearly adiabatic layer, where $\theta = 300$ K. The transition from the extremely high stability at the base of the stable region to the near-adiabatic region aloft is gradual. This structure characterizes soundings at 12 GMT 11 February, before the wave activity begins, and also CAR (Caribou, Maine) near the northern edge of the cloud shield at 12 GMT the next day.

These data are listed in Table 1 with comparable values from other relevant locations and times. Alternative choices are given for soundings with ambiguous layer tops. The calculated phase speeds, c, are shown in Table 1, and are corrected by subtracting the mean component from 050 deg, the direction toward which the system is propagating (Fig. 2), to yield the speed over the ground, c'. This mean component is the average over the depth of the stable layer, appropriate for the duct and also appropriate for the effective wind at an idealized discontinuity at the center of the stable layer.

Comparison between the phase speeds in Table 1 and the observed values, c^1 is difficult, because of paucity of soundings at just the right times and places. The comparisons at 12 GMT on the 11th and 12 GMT on the 12th are somewhat imaginary, as the wave has not yet appeared at the earlier time and has left the analysis area, and has probably dissipated, at the later time. The most appropriate single sounding, at ACY at 00 GMT on the 12th, unfortunately lacks wind data, but the mean northeasterly component in the stable layer was probably about 10 m s^{-1}.

Overall, the values of c_{inv} are too large, except perhaps in the 12 GMT data on the 11th. For both c_{inv} and c_{duct}, values for the deeper alternative layers are much larger than for the shallow layers, not only because of the greater values of $\theta_2 - \theta_1$, h, and H, but also because the opposing u, being averaged up to greater heights in a strongly sheared atmosphere, is much reduced. These values are also substantially larger than the observed speeds.

On the other hand, the values of c'_{duct}, using the shallower option when it is available, are too small but only slightly so after 12 GMT on the 11th. An exception, 30 m s^{-1} at PWM at 00 GMT on the 12th, is too far north and east for a convincing comparison with the wave speed at that time but may not be too large at the later time of passage of the system. A speed of 34 m s^{-1} for the rise center is indicated by Fig. 2p–r as it passes PWM.

Since the stable layer is saturated at most stations, a reduced Brunt–Väisälä frequency based on moist thermodynamics would be more appropriate than the dry-adiabatic value used in Table 1. The difference is not large, however. Calculations for the two warmest moist soundings, at GSO and at ACY show reductions of c_{inv} ranging from 2 to 6 m s^{-1} and from 1 to 4 m s^{-1}, respectively. The solitary character of the system, in at least some respects, suggests a cancelling error, moreover. Christie et al. (1978) in a review of classical

TABLE 1. Phase speeds through the air, c, and over the ground, c^1, from Eqs. (3) and (5) in m s^{-1}; u is wind component from 050 deg. See text for definition of other quantities. Asterisk means duct is unsaturated. Values in parenthesis refer to alternative specifications of the top of the stable layer (see text).

Station	1	2	H (m)	h (m)	c_{inv}	c_{duct}	u	c_{inv}^1	c_{duct}^1
				12 GMT 11 February ($c_{obs}^{-1} \leq 15$ m s^{-1}?)					
GSO	274	291 (300)	700 (2050)	1300 (1975)	28 (42)	13 (27)	14 (1)	14 (41)	−1 (26)
WAL	277	286 (298)	580 (3135)	1150 (1970)	19 (38)	9 (25)	12 (−2)	7 (40)	−3 (27)
IAD	268	288 (306)	1280 (4100)	1340 (2650)	31 (59)	19 (46)	12 (−1)	19 (60)	7 (34)
ACY	268	281 (296)	960 (2900)	1000 (1950)	21 (44)	13 (34)	10? (0?)	11? (34?)	3? (24?)
				00 GMT 12 February ($c_{obs}^1 \approx 20$ m s^{-1}?)					
ACY	274	299	1800	2400	45	25	10?	35?	15?
*CHH	270	292	1700	1750	37	23	10	27	13
*MIT	268	294	2100	2050	43	28	11	32	17
*PWM	265	297	3050	2255	50	37	7	43	30
				06 GMT 12 February ($c_{obs}^1 \geq 23$ m s^{-1})					
MIT	273	294	1500	2150	40	21	9	31	12
				12 GMT 12 February ($c_{obs}^1 > 23$ m s^{-1}?)					
PWM	261	295	3100	1900	48	39	17	31	22
WOS	264	302	3300	1850	49	42	10	38	32
*CAR	253	284 (300)	2100 (5250)	1250 (2825)	38 (69)	31 (60)	7 (2)	31 (62)	24 (58)

solitary wave theory, note that such nonlinear systems move at speeds which are slightly supercritical, i.e., faster than the speeds given for linear waves in equations (3) and (4). We conclude, therefore, that the Lindzen and Tung (1976) formula represents an improvement over (3) and is reasonably accurate when applied to a layer of distinctly large stability.

Other aspects of this case, moreover, make the view presented by these authors appealing. Where the wave is intense, there is both a suitable duct and, as seen in Sanders and Bosart (1985a), an elevated layer of small Richardson Number containing a critical level. [Despite the failure of the ACY winds at 00 GMT 12 February (Fig. 13) we know from the nearby IAD wind profile and geostrophic considerations that a critical level was still present above 400 mb as the wave became better organized and accelerated northeastward to a phase velocity of nearly 20 m s^{-1} (Figs. 3 and 7). The special 06 GMT 12 February MIT sounding (Fig. 9 of Sanders and Bosart, 1985a) indicates that the accelerating and slowly weakening wave had propagated out from under a critical layer aloft as the phase velocity of the wave became much greater than the wind within the inversion.] Thus, in Lindzen and Tung's (1976) terms, over-reflection can occur by extraction of energy from the mean flow. (Such an effect was suggested by Stobie et al., 1983, as well.) North of this region, upper winds are weaker and the upper stratification is stronger so that the vertically radiating waves are not effectively reflected. To the south of this region, over the ocean, the surface boundary layer must be warmer and deeper; we may thus speculate that a suitable duct does not exist. When the system accelerates northward and weakens, there is some evidence that the reflecting properties of the upper layer are becoming marginal.

The observed duct, unlike Lindzen and Tung's model, does not extend to the ground. The evanescent loss of wave amplitude in the shallow surface mixed layer, however, is not likely to be large (Lindzen, personal communication, 1985). Further, there appears to be no requirement for the vertical motion, w, to vanish at the base of the actual duct. Were the surface mixed layer simply (if perhaps improperly) regarded as part of the duct, so that w indeed vanishes at its base, then the duct thickness would be larger and the phase speed estimates improved.

8. Conclusions

We have studied a large-amplitude singular gravity wave through analysis of hourly observations, radar and satellite data, and observations of cloud-to-ground lightning flashes by the SUNYA network. The wave activity was initiated just ahead of, and to the left of, the track of a major cyclone which was responsible for the Megalopolitan snowstorm of 11–12 February 1983.

Hourly changes of sea level pressure up to several millibars accompanied the system, which first resembled a classic wave of depression. The pressure rises then increased to produce a wave of elevation, which was finally followed by a wake depression. The system propagated northeastward in the coastal region at 15 m s^{-1} accelerating to more than 25 m s^{-1}, against an increasing northeasterly flow at low levels. Its scale in the direction of propagation contracted upon organization to about 100 km, then expanded to more than 400 km as it accelerated during the remainder of the 12 hours over which it could be reliably tracked. The system period increased slowly from somewhat less to somewhat more than 3 hours.

Surface northeasterlies increased and became gusty with the approach of the first pressure falls, reaching a maximum at the pressure trough, then abruptly weakened and backed as strong pressure increases were observed. This behavior was in accord with a simple model of a gravity wave.

Strong fluctuations in column total condensation rate and radar reflectivity occurred with the passage of the wave, in qualitative agreement with the simple model. The effect could not be reliably detected in the surface snowfall observations, however, owing to difficulty in determining short-term fluctuations of snowfall rate in strong winds. Modest convective cloud buildups were triggered by the wave in potentially unstable air where a dry intrusion in middle-tropospheric levels had removed a continuous layer of deep high cloud.

Electrical activity was initiated by wave passage, but in discrete, sporadic clusters at intervals of about 3 hours. Each cluster tended to remain geographically fixed for 2–4 hours after initiation. The clusters occurred principally near the intersection of the gravity wave and the east–west oriented escarpment of deep high cloud along the north edge of the dry intrusion. These flashes carried predominantly negative charge to ground. A unique cluster of flashes developing from clouds with relatively low, warm tops, growing in the northern periphery of the dry intrusion, lowered exclusively positive charge to ground.

The first disorganized gravity-wave activity developed in the presence of modest convection just south of the mass of deep high cloud, and also beneath the region of likely wave generation in a strong shear zone beneath an advancing jet streak.

The singular-appearing large-amplitude wave became organized subsequently in a transient meridionally oriented zone of strong frontogenetical forcing that did not succeed in producing a surface front. Rather, the wave appeared as the northern extension of a front farther south reaching down to the low center.

The propagation speed of the system was in reasonable accord with the gravity-wave model of Lindzen and Tung (1976), but the theoretical speed was a few m s^{-1} slower than observed. Uncertainties in the interpretation of the structure of the ambient atmosphere and in the interpretation of the solitary aspects of the

wave were sufficient to account for the discrepancies. We conclude that the system represented a ducted gravity wave propagating in a layer of large stability beneath an elevated layer of small Richardson number containing a critical level. Whether the accompanying convection and enhancement of condensation heating represented a forcing effect on the wave is unknown because of uncertainties concerning its vertical structure, but circumstantial evidence indicates that the answer is probably yes.

Acknowledgments. We are pleased to acknowledge the benefit of conversation with D. R. Christie, Australian National University, Canberra, and R. S. Lindzen, MIT. We very much appreciate the interest and critical comments of K. A. Emanuel, MIT, J. Gyakum, University of Illinois, D. Lilly, University of Oklahoma, R. E. Passarelli, Sigmet Corp., and L. W. Uccellini, NASA-Goddard. Song C. Lin provided computational support. Prof. R. Orville kindly supplied the SUNYA lightning flash data and we appreciate his critical comments on the manuscript. The figures were drafted by Ms. Isabelle Kole and Mrs. Marilyn Peacock, while Ms. Kathy Stutsrim and Ms. Carol Tennant prepared the manuscript. The excitement and interest of SUNYA graduate students, past and present, in this case is greatly appreciated. This research has been supported by National Science Foundation Grants ATM-8026557 and ATM-8311106 (SUNYA), ATM-8019301 (MIT) and ATM-8407142 (SWE).

APPENDIX

A map showing the key locations and station letter designators used in the text is given in Fig. A1.

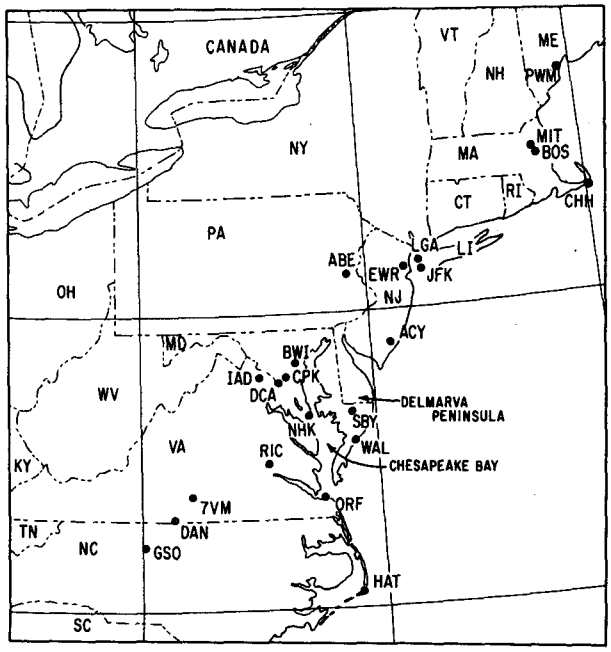

FIG. A1. Place locator and station letter designators for places mentioned in the text.

REFERENCES

Bjerknes, J., 1951: Extratropical cyclones. *Compendium of Meteorology,* T. F. Malone, Ed., Amer. Meteor. Soc., 577–598.

Bosart, L. F., and J. P. Cussen, Jr., 1973: Gravity wave phenomena accompanying East Coast cyclogenesis. *Mon. Wea. Rev.,* **101,** 446–454.

Brook, M., M. Nakano and P. Krehbiel, 1982: The electrical structure of the Hokuriku winter thunderstorms, *J. Geophys. Res.,* **87**(C2), 1207–1215.

Brunk, I., 1949: The pressure pulsation of 11 April 1944. *J. Meteor.,* **6,** 181–187.

Carlson, T. B., 1980: Airflow through midlatitude cyclones and the comma cloud pattern. *Mon. Wea. Rev.,* **108,** 1498–1509.

Christie, D. R., K. J. Muirhead and A. L. Hales, 1978: On solitary waves in the atmosphere. *J. Atmos. Sci.,* **35,** 805–825.

Eom, J., 1975: Analysis of the internal gravity wave occurrence of April 19, 1970 in the Midwest. *Mon. Wea. Rev.,* **103,** 217–226.

Ferguson, H. L., 1967: Mathematical and synoptic aspects of a small-scale wave disturbance over the lower Great Lakes area. *J. Appl. Meteor.,* **6,** 523–529.

Gedzelman, S. D., and W. L. Donn, 1979: Atmospheric gravity waves and coastal cyclones. *Mon. Wea. Rev.,* **107,** 667–681.

Gossard, E. E., and W. H. Munk, 1954: On gravity waves in the atmosphere. *J. Meteor.,* **61,** 259–269.

Green, J. S. A., R. H. Ludlam and J. F. R. McIlveen, 1966: Isentropic relative-flow analysis and the parcel theory. *Quart. J. Roy. Meteor. Soc.,* **92,** 210–219.

Hooke, W. H., and K. R. Hardy, 1975: Further study of the atmospheric gravity waves over the Eastern seaboard on 18 March 1969. *J. Appl. Meteor.,* **14,** 31–38.

Hoskins, B. J., and F. P. Bretherton, 1972: Atmospheric frontogenesis model: Mathematical formulation and solution. *J. Atmos. Sci.,* **29,** 11–37.

Ley, B. E., and W. R. Peltier, 1978: Wave generation and frontal collapse. *J. Atmos. Sci.,* **35,** 3–17.

Lindzen, R. S., and K. K. Tung, 1976: Banded convective activity and ducted gravity waves. *Mon. Wea. Rev.,* **104,** 12, 1602–1617.

Miller, D. G., and F. Sanders, 1980: Mesocale conditions for the severe convection of 3 April 1974 in the east-central US. *J. Atmos. Sci.,* **37,** 1041–1055.

Orville, R. E., R. W. Henderson and L. F. Bosart, 1983: An east coast lightning detection system. *Bull. Amer. Meteor. Soc.,* **64,** 1029–1037.

Pecnick, M. J., and J. A. Young, 1984: Mechanics of a strong subsynoptic gravity wave deduced from satellite and surface observations. *J. Atmos. Sci.,* **41,** 1850–1862.

Pothecary, I. J. W., 1954: Short-period variations in surface pressure and wind. *Quart. J. Roy. Meteor. Soc.,* **80,** 395–401.

Reed, R. J., and K. R. Hardy, 1972: A case study of persistent, intense, clear air turbulence in an upper level frontal zone. *J. Appl. Meteor.,* **11,** 541–549.

Sanders, F., and L. F. Bosart, 1985a: Mesoscale structure in the megalopolitan snowstorm of 11–12 February 1983. Part I: Frontogenetical forcing and symmetric instability. *J. Atmos. Sci.,* **42,** 1050–1061.

——, and ——, 1985b: Mesoscale structure in the megalopolitan snowstorm of 11–12 February 1983. Part II: Doppler radar study of the New England snowband. *J. Atmos. Sci.,* **42,** 1398–1407.

Saucier, W. J., 1955: Principles of Meteorological Analysis. University of Chicago Press, 438 pp.

Stobie, J. G., F. Einaudi and L. W. Uccellini, 1983: A case study of gravity waves—convective storm interaction: 9 May 1979. *J. Atmos. Sci.,* **40,** 2804–2830.

Takeuti, T., M. Nakano, M. Brook, D. J. Raymond and P. Krehbiel, 1978: The anomalous winter thunderstorms of the Hokuriku Coast. *J. Geophys. Res.,* **83, C5,** 2385–2394.

Uccellini, L. W., 1975: A case study of apparent gravity wave initiation of severe convective storms. *Mon. Wea. Rev.,* **103,** 497–513.

Wagner, A. J., 1962: Gravity wave in New England, April 12, 1961. *Mon. Wea. Rev.,* **90,** 431–436.